Chemical Physics Letters 573 (2013) 19–23

Contents lists available at SciVerse ScienceDirect

Chemical Physics Letters

journal homepage: www.elsevier.com/locate/cplett

Thermodynamic properties of carbon dioxide clusters by M06-2X and dispersion-corrected B2PLYP-D theory

Kono H. Lemke [a,*], Terry M. Seward [b,1]

[a] Department of Earth Sciences, University of Hong Kong, Pokfulam Road, Hong Kong SAR, China
[b] School of Geography, Environment and Earth Sciences, Victoria University of Wellington, New Zealand

ARTICLE INFO

Article history:
Received 7 March 2013
In final form 19 April 2013
Available online 27 April 2013

ABSTRACT

The M06-2X and B2PLYP-D functionals have been applied to predict structures and energies for $(CO_2)_n$ clusters up to $n = 16$. A comparison between M06-2X, B2PLYP-D and benchmark CCSD(T) results indicates that M06-2X is capable of providing accurate binding energies. Stepwise M06-2X $(CO_2)_n$ clustering free energies exhibit a sharp discontinuity at the magic cluster size $n = 13$ and systematically shift to more exergonic values with decreasing temperature, in particular for larger clusters. These results indicate that the M06-2X method provides an accurate and cost effective description of non-covalent interactions in $(CO_2)_n$ clusters and therefore may provide important information on CO_2 nucleation phenomena.

1. Introduction

Dispersion interactions play an important role in nature and are involved in the stabilization of a plethora of different molecular aggregates [1]. Carbon dioxide clusters $(CO_2)_n$ are a typical example in which monomers interact through dispersion. The ability to accurately describe these type of interactions is crucial in understanding fundamental molecular-scale processes controlling the chemistry of carbon dioxide. These weak interactions pose a special challenge for experimental techniques and are therefore in many cases either difficult or impossible to explore [2–4]. On the other hand, interaction energies of carbon dioxide complexes have been explored using both correlated second-order Møller–Plesset MP2 [5–8] and coupled cluster CCSD(T) theory [5,9] up to the complete basis set (CBS) limit level. However, high level correlation methods, such as CCSD(T) scale as the N^7 and are therefore computationally demanding. Given the cost of CCSD(T) and MP2 computations on larger molecular systems, there is a critical requirement for computationally less demanding methods that deliver results of comparable accuracy for large non-covalent chemical systems.

The density functional theory (DFT) approach is a widespread method for examining chemical systems with up to several hundred atoms, however, application of routine DFT to systems with non-covalent interactions has been restricted due the failure of most DFT methods, for instance, B3LYP and PW91, to accurately capture dispersion interactions [10]. While B3LYP and other popular DFT methods fail in describing dispersion interactions in non-covalent complexes, dispersion-corrected B2PLYP-D [11] and M06-2X functionals [12] have demonstrated excellent performance relative to high level correlated methods such as MP2 and CCSD(T) for a wide range of non-covalent interactions [13,14]. However, there are no DFT-D or M06-2X data currently available that would serve as a performance benchmark for predicting structures and energies of carbon dioxide clusters. In this study we examine stable structures and energies for $(CO_2)_n$ clusters up to $n = 16$ using M06-2X and the dispersion-corrected B2PLYP-D method. We compare our theoretical clustering energies with those predicted at the CCSD(T) level of theory and report DFT energies and thermodynamic properties for $(CO_2)_n$ clusters with $n \leqslant 16$.

2. Methods

In this study we have applied the recently developed Minnesota meta-exchange–correlation functional M06-2X, which has been specifically parametrized to capture medium-range dispersion interactions (up to 5 Å) [15] and therefore should be well-suited to describe dispersion-bound systems such as $(CO_2)_n$. In addition, we have conducted a survey of structures and energies of $(CO_2)_n$ clusters using dispersion-corrected B2PLYP-D theory [11]. In brief, the B2PLYP-D approach employs a damped semi-empirical R^{-6} dispersion term that is summed into the DFT energy. A detailed summary of the B2PLYP-D approach is given in Schwabe and Grimme [11]. All DFT $(CO_2)_n$ cluster calculations presented here incorporate a counterpoise (CP) correction for basis set superpositions error (BSSE). In order to benchmark our DFT clustering energies, we have evaluated the performance of M06-2X and B2PLYP-D against the hybrid B3PW91 functional and higher-level CCSD(T) computations for the carbon dioxide dimer and trimer. All $(CO_2)_n$ starting geometries with $2 \leqslant n \leqslant 16$ have been built in accord with structures

* Corresponding author. Fax: +852 2517 6912.
E-mail addresses: kono@hku.hk (K.H. Lemke), terry.seward@vuw.ac.nz (T.M. Seward).
[1] Fax: +64 04 463 5186.

0009-2614/$ - see front matter © 2013 Elsevier B.V. All rights reserved.
http://dx.doi.org/10.1016/j.cplett.2013.04.044

proposed by molecular dynamic simulations of carbon dioxide clusters [16]. Geometry optimizations, zero-point energy (ZPE) and thermal corrections have been calculated using the GAUSSIAN09 program [17] and the basis set applied in this study correspond to aug-cc-pVDZ for C and O.

3. Results and discussion

A comparison between various DFT (M06-2X, B2PLYP-D and B3PW91) and benchmark CCSD(T) cluster structures and binding energies for $(CO_2)_n$ with $n = 2$ and 3 are presented in Table 1, and optimized M06-2X/aug-cc-pVDZ structures for carbon dioxide clusters up to $n = 16$ are shown in Figure 1. A comparison between M06-2X and B2PLYP-D optimized geometries of the slipped parallel (C_{2h}) and T-shaped (C_{2v}) CO_2 dimer and those derived from CCSD(T)/aug-cc-pVDZ [9] suggests that both DFT functionals are able to predict structures that are in good agreement with high level ab initio computations (see Table 1). The DFT prediction for the C···C distance in the C_{2h} dimer is 3.380 Å for M06-2X and 3.494 Å for B2PLYP-D, and these values, in particular DFT-D results, compare well with higher level CCSD(T)/aug-cc-pVDZ (3.463 Å). The C···O distance between CO_2 monomers in the C_{2v} dimer predicted by CCSD(T)/aug-cc-pVDZ is 2.932 Å, while DFT predictions are 2.886 Å (M06-2X) and 2.950 Å (B2PLYP-D). The CCO angle (θ) between the monomers in the slipped parallel dimer is 59.4° with M06-2X and 59.5° with B2PLYP-D, while θ is 58.1° with CCSD(T)/aug-cc-pVDZ.

In general, good agreement was found between DFT and CCSD(T) results [5] for the optimized structures of the cyclic (C_{3h}) and non-cyclic (C_2) CO_2 trimers. The M06-2X and B2PLYP-D distances between the CO_2 carbon atoms in the cyclic trimer are 3.834 and 3.998 Å, respectively, while the CCSD(T) value is 4.01 Å. The monomer orientation angle β in the cyclic trimer is 39.2° at the M06-2X level of theory and 39.0° with the B2PLYP-D method, which, for reference, is very close to the CCSD(T) value of 39.1°. The out-of-plane tilt angles γ in the cyclic trimer predicted by M06-2X and B2PLYP-D are 0° and exactly match results predicted by CCSD(T) theory [5]. The distance between both basal CO_2 carbon atoms in the C_2 trimer is predicted to be 3.533 Å with M06-2X and 3.627 Å with B2PLYP-D. This distance is calculated to be 3.737 Å at the CCSD(T) level and a slightly longer distance, 3.761 Å, is found by experiment [18]. The DFT predictions for the out-of-plane tilt angle γ in the non-cyclic C_2 trimer are 12.0° and 11.9° for M06-2X and B2PLYP-D, respectively, and these values are very close to the CCSD(T) level value of 11.5°.

Figure 1 presents M06-2X/aug-cc-pVDZ optimized structures of CO_2 clusters up to the $n = 16$. In brief, M06-2X structures of $(CO_2)_n$ presented here closely match results from IR spectroscopic experiments [19,20]. Recent rotational spectroscopic work [20] has indicated that the CO_2 tetramer is a trigonal pyramidal structure, while the CO_2 pentamer is a trigonal bipyramid with a central ring in which all three CO_2 monomers are tilted out-of-plane. High resolution IR spectroscopic studies of the CO_2 hexamer [19] have identified two highly symmetric CO_2 hexamers: one that is formed by stacking two cyclic trimers (S_6) and a tetragonal bipyramidal structure (S_4) consisting of a four-membered ring capped by two monomers (see Figure 1). The CO_2 heptamer has been proposed to be a highly asymmetrical cluster consisting of a pentagonal ring and two CO_2 monomers positioned along the *c*-axis above and below the ring [19]. There are, to our knowledge, no experimental results for the structures of $(CO_2)_8$, however, Takeuchi [16] has shown, using empirical potentials, that the CO_2 octamer is another highly asymmetric structure with five CO_2 molecules arranged in a ring, with two CO_2 monomers above and one CO_2 monomer below the ring. For larger CO_2 clusters, i.e. with $n = 9$–16, the most stable cluster structures are derived from a 3–6–3 ring motif, composed of a staggered equatorial ring of six monomers capped by two rings of three CO_2 monomers with one centrally enclosed CO_2 monomer ($n = 13$); this motif is also conserved in larger CO_2 clusters, in other words, CO_2 clusters with $n = 14$, 15 and 16 are built by packing CO_2 monomers onto the surface of the CO_2 tridecamer. In general, the structures of $(CO_2)_n$ clusters are well-known, thus this study will focus primarily on the stepwise DFT binding energies and thermodynamic properties of individual CO_2 clustering reactions. In view of the importance of CO_2 clusters as a typical system driven by dispersion–driven interactions and their perceived relevance in atmospheric chemistry and CO_2 cloud nucleation [21] we have evaluated, by M06-2X and B2PLYP-D level theory, the energies and thermodynamic properties of $(CO_2)_n$ in the size range $2 \leqslant n \leqslant 16$.

Table 1 lists a comparison between DFT and CCSD(T) benchmark binding energies for $(CO_2)_n$ with $n = 2$, 3; these data are further expanded in Table 2 and Figure 2 to include stepwise and total M06-2X/aug-cc-pVDZ level $(CO_2)_n$ clustering energies, enthalpies, entropies and the temperature-dependance of the free energy change up to $n = 16$. The uncorrected electronic binding energy ΔE_e for the slipped-parallel C_{2h} dimer is predicted to be −1.47 kcal/mol at the M06-2X level and −1.56 kcal/mol using the B2PLYP-D approach; the DFT binding energies for the T-shaped dimer are consistently smaller than that for the slipped-parallel dimer (~0.3–0.4 kcal/mol less). For comparison, the CCSD(T)/aug-cc-pVDZ binding energy is −1.86 kcal/mol (C_{2h}) and −1.64 kcal/mol (C_{2v}) [9], which is around 20% and 16% more than for the M06-2X and B2PLYP-D approach, respectively. The M06-2X and B2PLYP-D total binding energies for the cyclic C_{3h} trimer are −4.08 and −4.19 kcal/mol, while DFT predictions for the stacked noncyclic C_2 trimer are slightly larger, −4.15 kcal/mol with M06-2X and −4.26 kcal/mol with B2PLYP-D; a slightly smaller C_{3h} binding energy, −4.02 kcal/mol, and C_2 binding energy, −4.11 kcal/mol, is predicted with CCSD(T) theory [5]. It would appear that the B2PLYP-D approach moderately underestimates the trimer binding energy, relative to CCSD(T), while M06-2X binding energies are sufficiently close to CCSD(T) making this DFT method suitable for studying large CO_2 cluster. Furthermore, since B2PLYP-D calculations are prohibitively expensive relative to M06-2X, we suggest that the later DFT method be used for calculations of larger $(CO_2)_n$ clusters. Table 1 also lists geometric parameters and binding energies of CO_2 clusters calculated at the B3PW91/aug-cc-pVDZ level of theory. Not surprisingly, the B3PW91 functional fails to

Table 1
Optimized geometric parameters and electronic binding energies (ΔE_e) in kcal/mol for $(CO_2)_n$ with $n = 2$, 3.

Cluster			CCSD(T)	B3PW91	M06-2X	B2PLYP-D
$n = 2$	C_{2h}	$R_{C\cdots C}$	3.463 Å[a] 3.503 Å[b]	4.698 Å	3.380 Å	3.494 Å
		Θ	58.1[a] 58.9[b]	53.4°	59.4°	59.5°
		ΔE_e	−1.86[a] −1.49[b]	−0.57	−1.47	−1.56
	C_{2v}	R_{C-O}	2.932 Å[a] 2.949 Å[b]	3.818 Å	2.886 Å	2.950 Å
		ΔE_e	−1.64[a] −1.20[b]	−0.19	−1.20	−1.01
$n = 3$	C_{3h}	$R_{C\cdots C}$	4.01 Å[c]	4.841 Å	3.834 Å	3.998 Å
		ΔE_e	−4.02 [c]	−0.57	−4.08	−4.19
		β	39.1°[c]	40.6°	39.2°	39.0°
	C_2	$R_{C\cdots C}$	3.737 Å[c]	5.628 Å	3.533 Å	3.627 Å
		ΔE_e	−4.11[c]	−0.39	−4.15	−4.26
		γ	11.5°[c]	16.5°	12.0°	11.9°

[a] CCSD(T)/aug-cc-pVDZ.
[b] CCSD(T)/CBS [9].
[c] CCSD(T)/6-311G* [5].

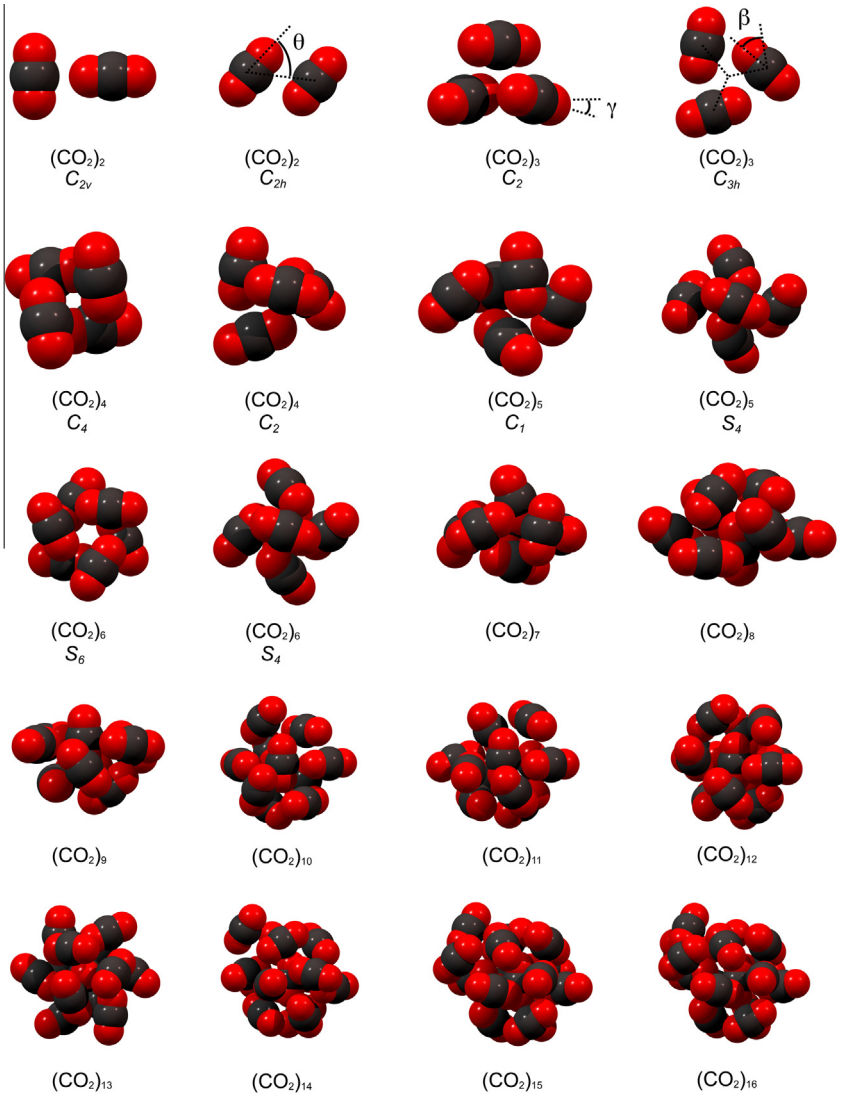

Figure 1. M06-2X/aug-cc-pVDZ minimum energy structures of carbon dioxide clusters $(CO_2)_n$ with $n = 2–16$.

predict the correct cluster structures and binding energies, which is due to a well-known deficiency in the long range behavior of this functional [22]. Thus, for dispersion bound systems such as $(CO_2)_n$ B3PW91 should be avoided in favor of M06-2X and B2PLYP-D.

The M06-2X/aug-cc-pVDZ stepwise and total binding energies (ΔE_o), before and after CP and ZPE correction, enthalpies (ΔH_{298K}), entropies (ΔS_{298K}) and free energies (ΔG) at 5, 50, 150 and 298 K for CO_2 clustering reactions are summarized in Table 2, and Figure 2 presents the results graphically. The largest discontinuity in the stepwise reaction enthalpy and entropy occurs at $n = 13$, with three more moderate discontinuities in the $\Delta H°$ and $\Delta S°$ profile at $n = 4$, 7 and 9. The stepwise M06-2X enthalpy values for carbon dioxide clusters from $n = 8$ onward to $n = 12$ decrease significantly slower (by around 0.1–0.3 kcal/mol), in other words, these structures exhibit no special stability. On the other hand, the large negative enthalpy value at $n = 13$ ($\Delta H°_{12,13} = -4.32$ kcal/mol) and reduced entropy contribution at 298 K ($T\Delta S°_{12,13} = -7.74$ kcal/mol) to $\Delta G°$, can best be explained by invoking a magic-number $(CO_2)_{13}$ cluster with enhanced stability [16]. The observed enthalpy and entropy discontinuity at $n = 13$ corresponds to the completion of a full $(CO_2)_{13}$ cluster (see Figure 1), and thus, the enthalpy and entropy values for higher CO_2 clustering reactions are less pronounced because subsequent CO_2 molecules attach to outer surface of the magic cluster where bonding is anticipated to be weaker. Also shown in Figure 2 are the M06-2X stepwise values of $\Delta G°$ for the reaction $(CO_2)_{n-1} + CO_2 = (CO_2)_n$ in the temperature range 50–298 K, and we can see that for $n = 13$ $\Delta G°$ drops to negative values below around 160 K, pointing to a favorable growth of CO_2 clusters with decreasing temperature. This trend, for $n = 13$, continues as the temperature is further reduced from 150 K ($\Delta G° = -0.42$ kcal/mol), 50 K ($\Delta G° = -3.02$ kcal/mol) to 5 K ($\Delta G° = -4.19$ kcal/mol) (see Table 2). Figure 2 shows that, starting at around 100 K, the clustering free energies $\Delta G°$ for $n = 6–15$ systematically decrease (i.e. shift to exergonic values) with decreasing temperature, and the formation of larger clusters with $n = 12–16$ at 50 K seems to be particularly pronounced. In general, the trends in $\Delta G°$ point towards a favorable stepwise assembly of carbon dioxide clusters at lower temperatures, but not at temperatures above 150 K. The magic cluster $(CO_2)_{13}$ however, has a negative $\Delta G°$ value at 150 K, and therefore would form from a precursor $(CO_2)_{12}$ cluster.

4. Conclusion

This study shows that the B2PLYP-D functional is able to predict geometries of carbon dioxide dimers (C_{2h} and C_{2v}) and trimers (C_{3h} and C_2) that are in good agreement with benchmark CCSD(T) the-

Table 2
M06-2X/aug-cc-pVDZ stepwise and total changes in the electronic energy (ΔE), enthalpy (ΔH_{298K}), entropy (ΔS_{298K}) and free energy (ΔG) in kcal/mol at 5, 50, 150 and 298 K and 1 bar.

n	ΔE_e[a]	ΔE_e[b]	ΔE_o[c]	ΔH_{298K}	ΔS_{298K}	ΔG_{5K}	ΔG_{50K}	ΔG_{150K}	ΔG_{298K}
Incremental energies; $(CO_2)_{n-1} + CO_2 = (CO_2)_n$									
2, C_{2h}	−1.47	−1.28	−0.88	−0.65	−18.13	−0.56	0.26	2.07	4.76
3, C_{3h}	−2.61	−2.16	−1.72	−1.29	−24.60	−1.16	−0.06	2.40	6.05
4, C_2	−3.88	−3.33	−2.74	−2.43	−25.02	−2.31	−1.18	1.32	5.02
5, C_1	−4.12	−3.40	−2.59	−2.46	−35.85	−2.29	−0.67	2.91	8.22
6, S_6	−4.27	−3.46	−2.77	−2.45	−33.60	−2.28	−0.77	2.59	7.57
7	−4.73	−4.08	−3.32	−3.21	−28.98	−3.06	−1.76	1.14	5.43
8	−4.30	−3.58	−2.93	−2.66	−30.01	−2.51	−1.16	1.84	6.29
9	−4.65	−3.81	−3.23	−2.89	−28.65	−2.75	−1.46	1.41	5.65
10	−4.49	−3.71	−3.10	−2.81	−31.16	−2.66	−1.26	1.86	6.48
11	−4.99	−4.07	−3.13	−3.05	−32.21	−2.88	−1.44	1.79	6.56
12	−5.28	−4.25	−3.47	−3.26	−30.73	−3.11	−1.72	1.35	5.90
13	−6.65	−5.22	−4.68	−4.32	−25.97	−4.19	−3.02	−0.42	3.42
14	−3.39	−3.27	−2.65	−2.36	−32.49	−2.19	−0.73	2.52	7.33
15	−5.41	−4.44	−3.76	−3.57	−31.75	−3.41	−1.98	1.19	5.90
16	−5.38	−4.37	−3.21	−3.37	−41.18	−3.17	−1.31	2.81	8.91
Total energies; $n(CO_2) = (CO_2)_n$									
2, C_{2h}	−1.47	−1.28	−0.88	−0.65	−18.13	−0.56	0.26	2.07	4.76
3, C_{3h}	−4.08	−3.45	−2.59	−1.94	−42.73	−1.72	0.20	4.47	10.81
4, C_2	−7.96	−6.78	−5.33	−4.37	−67.75	−4.03	−0.98	5.79	15.83
5, C_1	−12.08	−10.17	−7.92	−6.83	−103.60	−6.32	−1.65	8.70	24.05
6, S_6	−16.35	−13.63	−10.69	−9.28	−137.20	−8.60	−2.42	11.30	31.62
7	−21.08	−17.71	−14.01	−12.49	−166.18	−11.66	−4.18	12.44	37.06
8	−25.38	−21.29	−16.94	−15.15	−196.20	−14.17	−5.34	14.28	43.34
9	−30.03	−25.10	−20.17	−18.04	−224.85	−16.92	−6.80	15.68	49.00
10	−34.51	−28.81	−23.27	−20.86	−256.01	−19.58	−8.06	17.54	55.47
11	−39.51	−32.88	−26.41	−23.90	−288.22	−22.46	−9.49	19.33	62.03
12	−44.79	−37.14	−29.88	−27.16	−318.94	−25.57	−11.22	20.68	67.93
13	−51.43	−42.36	−34.56	−31.48	−344.91	−29.76	−14.23	20.26	71.36
14	−54.83	−45.63	−37.21	−33.84	−377.40	−31.95	−14.97	22.77	78.69
15	−60.24	−50.07	−40.97	−37.41	−409.15	−35.36	−16.95	23.97	84.58
16	−65.62	−54.44	−44.18	−40.78	−450.33	−38.53	−18.26	26.77	93.49

[a] Electronic binding energy.
[b] CP corrected electronic binding energy.
[c] CP and ZPE corrected electronic binding energy.

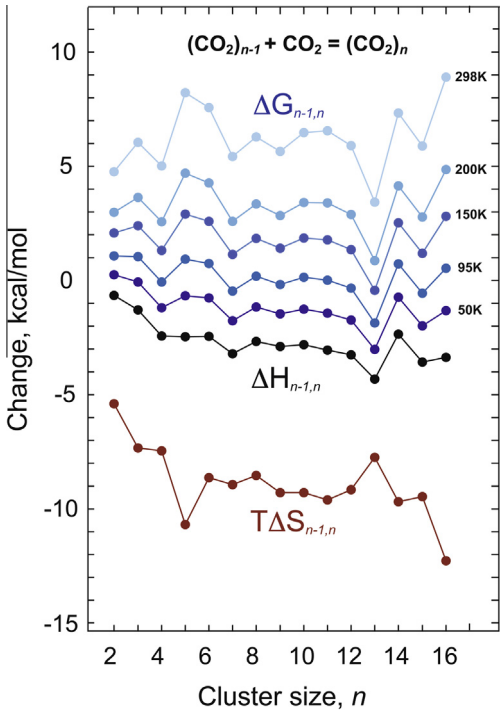

Figure 2. M06-2X/aug-cc-pVDZstepwise energy changes associated with the growth of small carbon dioxide clusters; values of $\Delta H_{n-1,n}$, $T\Delta S_{n-1,n}$ and $\Delta G_{n-1,n}$ correspond to the stepwise enthalpy, temperature-weighted entropy and temperature-dependent free energy change, respectively.

ory. M06-2X predictions of $(CO_2)_2$ and $(CO_2)_3$ cluster structures reveal only slightly shorter intermolecular distances. As for $(CO_2)_2$ and $(CO_2)_3$ binding energies, B2PLYP-D values tend to be underbound relative to CCSD(T) results, while the M06-2X approach provides binding energies that are consistently closer to the coupled cluster benchmark energies. Thus, M06-2X in combination with aug-cc-pVDZ offers a satisfactory description of the interactions among molecules in CO_2 clusters and can therefore be extended to significantly larger systems than accessible with B2PLYP-D, MP2 or CCSD(T) methods. The calculated CO_2 clustering enthalpies and entropies predict that the formation of $(CO_2)_n$ with $n = 2–16$ is unfavorable at 298 K, however, at lower temperatures ($T < 150$ K) the magic cluster $n = 13$ will form, and starting at around $T = 100$ K, clustering free energies for $n = 6–16$ shift to negative values, suggesting that $(CO_2)_n$ cluster growth is increasingly favorable with decreasing temperature. In general, the M06-2X approach provides a more accurate description of weakly bound carbon dioxide clusters, and thus may achieve high accuracy energies for larger clusters at a fraction of the cost of B2PLYP-D. This cost factor will become more significant for larger clusters because B2PLYP-D scales as N^5 whereas M06-2X scales as N^3.

Acknowledgments

Computing time was provided by the HKU High Performance Computing (HPC) and Grid Computing Centers. This project was supported in part by a Hong Kong UGC Special Equipment Grant (SEG HKU09) and General Research Fund HKU 702608P.

Appendix A. Supplementary data

Supplementary data associated with this article can be found, in the online version, at http://dx.doi.org/10.1016/j.cplett.2013.04.044.

References

[1] P. Hobza, K. Müller-Dethlefs, Non-Covalent Interactions, Theory and Experiment, RSC, Cambridge, 2009.
[2] J.M. Calo, J.H. Brown, J. Chem. Phys. 61 (1974) 3931.
[3] M. Yamashita, T. Sano, S. Kotake, J.B. Fenn, J. Chem. Phys. 75 (1981) 5355.
[4] F. Huisken, L. Ramonat, V.V. Smirnov, O.M. Stelmakh, A.A. Vigasin, CARS spectroscopy of carbon dioxide associating in free jet expansions, in: High Resolution Molecular Spectroscopy: 11th Symposium and School, International Society for Optics and Photonics, 1994, pp. 95–108.
[5] S. Tsuzuki, W. Klopper, H.P. Lüthi, J. Chem. Phys. 111 (1999) 3846.
[6] K.V. Jose, S.R. Gadre, J. Chem. Phys. 128 (2008) 124310.
[7] S.D. Yeole, N. Sahu, S.R. Gadre, Phys. Chem. Chem. Phys. 14 (2012) 7718.
[8] M.M. Deshmukh, S. Sakaki, J. Comput. Chem. 33 (2012) 617.
[9] J.D. McMahon, J.R. Lane, J. Chem. Phys. 135 (2011) 154309.
[10] S. Tsuzuki, H.P. Lüthi, J. Chem. Phys. 114 (2001) 3949.
[11] T. Schwabe, S. Grimme, Phys. Chem. Chem. Phys. 9 (2007) 3397 (B2PLYP-D).
[12] Y. Zhao, D.G. Truhlar, Theor. Chem. Acc. 120 (215) (2008) (M06-2X).
[13] Y. Zhao, D.G. Truhlar, J. Chem. Theory Comput. 4 (2008) 1849.
[14] E.G. Hohenstein, S.T. Chill, C.D. Sherrill, J. Chem. Theory Comput. 4 (2008) 1996.
[15] Y. Zhao, N.E. Schultz, D.G. Truhlar, J. Chem. Theory Comput. 2 (2006) 364.
[16] H. Takeuchi, J. Phys. Chem. A 112 (2008) 7492.
[17] M.J. Frisch et al., Gaussian 09, Revision C.01, Gaussian, Inc., Wallingford, CT, 2010.
[18] M.J. Weida, D.J. Nesbitt, J. Chem. Phys. 105 (1996) 10210.
[19] J.N. Oliaee, M. Dehghany, A.R.W. McKellar, N. Moazzen-Ahmadi, J. Chem. Phys. 135 (2011) 044315.
[20] M. Dehghany, A.R.W. McKellar, M. Afshari, N. Moazzen-Ahmadi, Mol. Phys. 108 (2010) 2195.
[21] F. Forget et al., Icarus 222 (2013) 81.
[22] M. Swart, M. Solà, F.M. Bickelhaupt, J. Comput. Chem. 32 (2011) 1117.